

The optical afterglow of the short gamma-ray burst associated with GW170817

J. D. Lyman¹, G. P. Lamb², A. J. Levan¹, I. Mandel³, N. R. Tanvir⁴, S. Kobayashi², B. Gompertz¹, J. Hjorth⁵, A. S. Fruchter⁶, T. Kangas⁶, D. Steeghs¹, I. A. Steele², Z. Cano⁷, C. Copperwheat², P.A. Evans⁴, J.P.U. Fynbo⁵, C. Gall⁵, M. Im⁸, L. Izzo⁷, P. Jakobsson⁹, Milvang-Jensen, B.⁵, P. O'Brien⁴, J.P. Osborne⁴, E. Palazzi¹⁰, D.A. Perley², E. Pian¹⁰, S. Rosswog¹¹, A. Rowlinson¹², S. Schulze¹³, E.R. Stanway¹, P. Sutton¹⁴, C.C. Thöne⁷, A. de Ugarte Postigo^{7,5}, D.J. Watson⁵, K. Wiersema¹ & R.A.M.J. Wijers¹⁵

¹*Department of Physics, University of Warwick, Coventry, CV4 7AL, UK*

²*Astrophysics Research Institute, LJMU, IC2, Liverpool Science Park, 146 Brownlow Hill, Liverpool L3 5RF, UK*

³*Birmingham Institute for Gravitational Wave Astronomy and School of Physics and Astronomy, University of Birmingham, Birmingham, B15 2TT, UK*

⁴*Department of Physics and Astronomy, University of Leicester, LE1 7RH, UK*

⁵*Dark Cosmology Centre, Niels Bohr Institute, University of Copenhagen, Juliane Maries Vej 30, Copenhagen Ø, 2100, Denmark*

⁶*Space Telescope Science Institute, 3700 San Martin Drive, Baltimore, MD 21218, USA*

⁷*Instituto de Astrofísica de Andalucía (IAA-CSIC), Glorieta de la Astronomía, s/n, 18008, Granada, Spain*

⁸*Center for the Exploration of the Origin of the universe (CEO), Seoul National University, Seoul, Korea; Astronomy Program, Department of Physics & Astronomy, Seoul National University, Seoul, Korea*

⁹*Centre for Astrophysics and Cosmology, Science Institute, University of Iceland, Dunhagi 5, 107 Reykjavík, Iceland*

¹⁰*INAF, Institute of Space Astrophysics and Cosmic Physics, Via Gobetti 101, I-40129 Bologna, Italy*

¹¹*The Oskar Klein Centre, Department of Astronomy, AlbaNova, Stockholm University, SE-106 91 Stockholm, Sweden*

¹²*Anton Pannekoek Institute, University of Amsterdam, Postbus 94249, 1090 GE Amsterdam, The Netherlands*

¹³*Department of Particle Physics and Astrophysics, Weizmann Institute of Science, Rehovot 761000, Israel*

¹⁴*School of Physics and Astronomy, Cardiff University, Cardiff, United Kingdom, CF24 3AA*

¹⁵*Anton Pannekoek Institute for Astronomy, University of Amsterdam, Postbus 94249, NL-1090 GE Amsterdam, the Netherlands*

The binary neutron star merger GW170817 was the first multi-messenger event observed in both gravitational and electromagnetic waves.^{1,2} The electromagnetic signal began ~ 2 seconds after the merger with a weak, short burst of gamma-rays,³ which was followed over the course of the next hours and days by the ultraviolet, optical and near-infrared emission from a radioactively-powered kilonova.⁴⁻¹¹ The low luminosity of the gamma-rays and the rising radio and X-ray flux from the source at late times could indicate that we are viewing this event outside the opening angle of the beamed relativistic jet launched during the merger. Alternatively, the emission could be arising from a cocoon of material formed from the interaction between a (possibly choked) jet and the merger ejecta.¹²⁻¹⁴ Here we present late-time optical detections and deep near-infrared limits on the emission from GW170817 at 110 days after the merger. Our new observations are at odds with expectations of late-time emission from kilonova models, being too bright and blue.^{15,16} Instead, this late-time optical emission arises from the optical afterglow of GRB 170817A, associated with GW170817. This emission matches the expectations of a structured relativistic jet, that would have launched a high luminosity short GRB to an aligned observer. The distinct predictions for the future optical behaviour in the structured-jet and cocoon models will directly distinguish the origin of the emission.

The gravitational-wave detection of the binary neutron star merger GW170817 in coincidence with the short duration gamma-ray burst GRB 170817A on 17 August 2017^{1,3} led to a major follow-up campaign across the electromagnetic spectrum.² These observations identified the counterpart in the galaxy NGC 4993,^{5,11} and showed that the early optical and infrared (IR) light was dominated by kilonova emission.⁴⁻¹¹ At later times, non-thermal X-ray and radio emission was also observed.^{12,17} The source was intensively monitored for the following month, but then its position on the sky became too closely aligned to the Sun for ultraviolet, optical, IR and X-ray observations.

For the Hubble Space Telescope (*HST*), the end of Sun constraint was on 6 December 2017 (~ 110 rest-frame days post-merger), and we immediately obtained deep observations in the optical and infrared (see Table 1 and Methods for details of the observations and reduction). The new images were astrometrically aligned to our earlier epoch *HST* data^{10,18} in order to accurately locate the merger site and perform photometry (see Methods). Images of the merger site in each of our filters are shown in Figure 1. We detect emission at the location of the merger in the optical F606W and F814W filters (central wavelengths, $\lambda_{\text{cen}} \sim 589, 802$ nm, respectively). For the near-IR filters F140W and F160W ($\lambda_{\text{cen}} \sim 1392, 1527$ nm, respectively) we could not establish significant detections and so can place only upper limits on the transient flux at these wavelengths. Optical and near-infrared light curves for the counterpart to GW170817, including our recent observations, are shown in Figure 2.

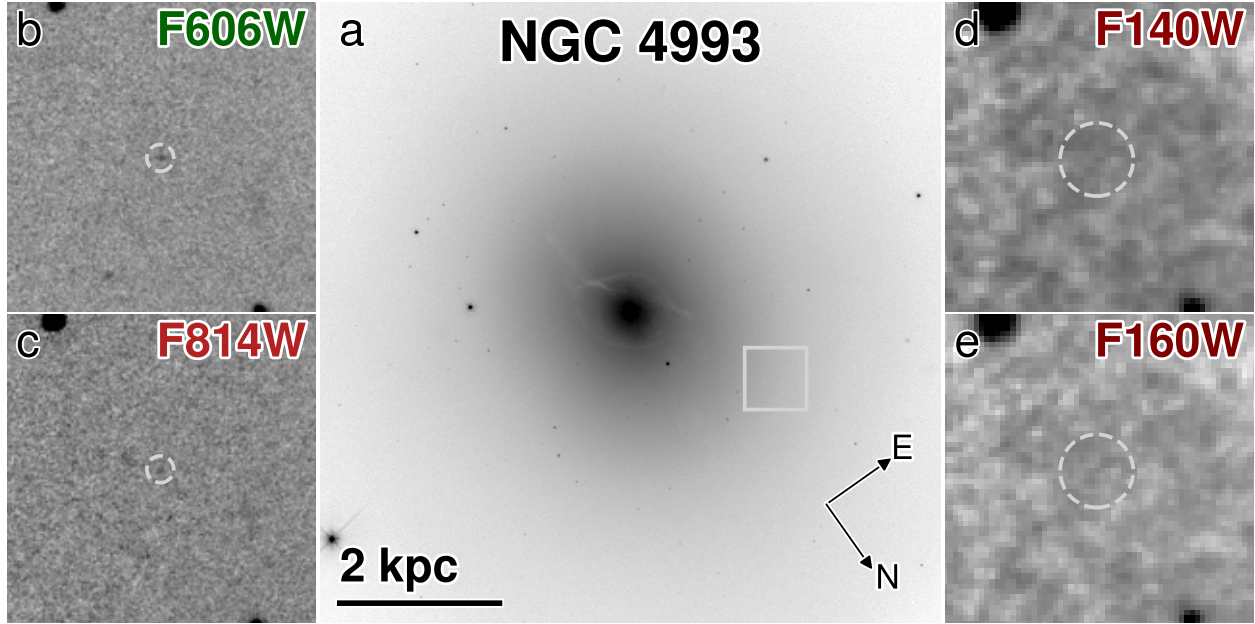


Figure 1 Late-time Hubble Space Telescope/Wide Field Camera 3 optical and near-infrared images of GW170817. The host galaxy, NGC 4993 is shown in F606W (a). Orientation and linear scale are indicated, as well as the region covered by the zoom-in panels. The merger site in each filter, as indicated, are shown (b-e). The dashed circles (radii $\simeq 2.5 \times \text{FWHM}$) are centered on our determined location of GW170817 in each case. The zoom-in panels have had the underlying galaxy background light subtracted (see Methods). We find significant detections in F606W and F814W but only upper limits on the flux in F140W and F160W.

A detection in the optical or near-IR at such late times is not expected from the family of kilonova models currently in use. Indeed, most detailed studies stop at ~ 30 days where predicted luminosities correspond to $\gtrsim 30$ mag,^{15,19} undetectable for even *HST*. Alternative models of kilonova emission with a slower decay of the light curves¹⁶ would nevertheless predict redder emission than we observe. Initially blue, with $M_{r,AB} - M_{H,AB} \simeq 0.4$ mag¹ at 1.5 days²⁰, GW170817 evolved to become very red, with $M_{F606W,AB} - M_{F160W,AB} = 2.8$ mag at 11 days post-merger¹⁰, consistent with optical line blanketing in the lanthanide-rich ejecta. Our late time detections and limits imply a much bluer colour at 110 days of $M_{F606W,AB} - M_{F160W,AB} \lesssim 1.5$ mag. Such evolution from blue to red and back to blue is not expected from current kilonova models. We note that this colour is bluer than that of typical globular clusters, and the source fainter than the majority of them. We consider our detections as being due to the transient and not an underlying source, although longer term optical monitoring will rule conclusively (see Supplementary Information).

Instead, we consider our observations in light of the radio and X-ray detections of the non-thermal GRB afterglow radiation. This synchrotron radiation is produced by relativistic electrons

¹*r* and *H* are ground-based filters, which are roughly comparable to our *HST* F606W and F160W observations.

gyrating in a magnetic field. The electrons in the interstellar medium around the merger may be accelerated to relativistic velocities by shocks arising from either a collimated, initially ultra-relativistic jet or a more isotropic, mildly relativistic ‘cocoon’. Early X-ray non-detections made with the *Swift* satellite,⁶ followed by later detections of rising radio and X-ray flux,^{12,14,17} indicate that either the jet is being viewed off-axis, or that the jet is unable to punch through the dynamical ejecta from the merger and the cocoon model is correct.^{12,13,21} The continued gradual rise of the radio flux from 15 to more than 100 days is difficult to reconcile with a classical ‘top-hat’ jet profile viewed off-axis, which would be expected to have a steeper rise (see Supplementary Information). A ‘top-hat’ jet has a homogeneous energy distribution within the jet opening angle, which sharply drops outside the jet. In reality, jets are unlikely to show this morphology and several structured jet models have been proposed.^{22–24} The temporal behaviour of the afterglow light curve from a decelerating structured jet depends on the specific structure model and viewing angle.²⁵

Here we show that the available radio, optical and X-ray afterglow emission can be well modelled by a relativistic jet with Gaussian structured morphology, chosen as a simple representation of a structured jet profile (see Supplementary Information). Model parameters producing a good match to the data are given in Table 2 and the resulting light curve and spectra at the epochs with the best observational constraints on the afterglow are shown in Figure 3. The continued rise of the radio and X-ray light curves from early to late times are well reproduced by the model. The late-time optical detections, near-IR limits and inferred radio-optical-X-ray spectral energy distribution we present here are also in good agreement with the model. The model suggests that the earlier optical and near-IR photometry was completely dominated by the kilonova light, with the contribution of the afterglow being $\gtrsim 29$ mag (see Figure 2). Unlike Ref. ¹³, where the jet is choked by the merger ejecta that powers a cocoon of material in the favored model, we find that the afterglow can be explained by an off-axis viewing angle of a highly relativistic jet.²⁶ If viewed close to on-axis, this jet would have an isotropic equivalent energy typical for other short GRBs (see Supplementary Information).

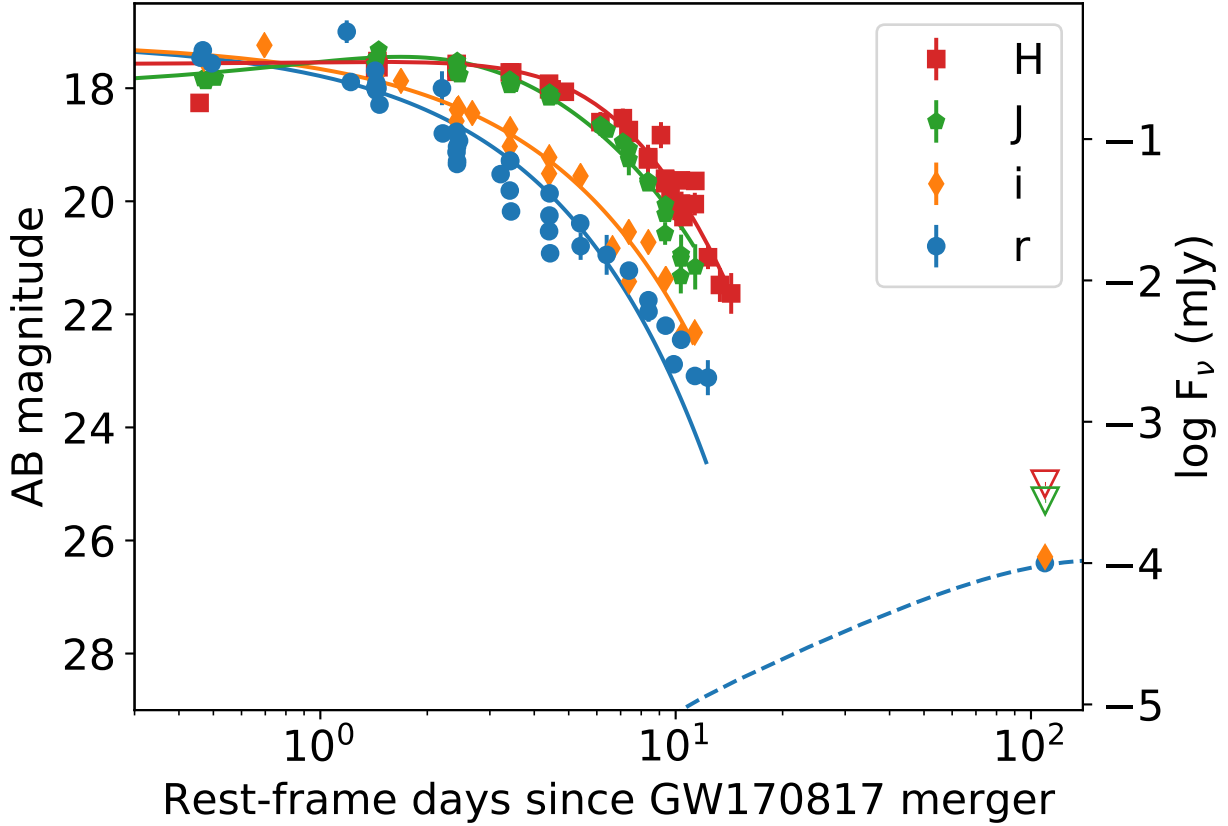


Figure 2 Optical and near-infrared light curve of GW170817. Multiwavelength light curves of the counterpart of GW170817 including our new late time measurements (in the colour and marker of the most similar ground-based photometric filter; near-IR 3σ limits are shown as open downward triangles). Earlier epochs are dominated by kilonova light, however the latest optical detections are much brighter and bluer than what is expected from kilonova models. The solid lines show the results of fitting an exponentially rising and decaying phenomenological function²⁷ to the early light curves.²⁸ The dashed line shows our structured jet afterglow in filter F606W ($\simeq r$). Error bars indicate 1σ uncertainties. Earlier photometry has been previously published^{4,5,8,10,11,20,29–31} and was taken from <https://kilonova.space>.³²

Thus, our interpretation does not require the introduction of a new class of choked-jet events to explain GW170817, and instead makes this event consistent with arising from the same population of observed on-axis short GRBs.³³

While our observations and modelling are consistent with an afterglow arising from a highly collimated jet, equally, we cannot rule out (or contradict) the existence of a cocoon. The exact

mechanism of how a jet develops its structure is unclear (as is jet formation itself). Ideal magnetohydrodynamic simulations show that neutron star mergers can self-consistently produce jets along the binary rotation axis.³⁴ In this setting, a jet forms and expands in a centrifugally evacuated low-density funnel, therefore the jet may not have significant interaction with any ejecta, and may not result in a cocoon. The jet’s structure in this case would be due to the intrinsic formation and acceleration mechanism. In nature, however, the jet will likely have to drill through earlier ejected matter produced by neutrino-driven winds³⁵ and/or shock-heated dynamical ejecta from the merger. This interaction shapes the structure of the jet. In this scenario, a cocoon will form that helps collimate the jet,³⁶ and as it emerges from the ejecta it will gain structure due to the jet-cocoon interaction³⁷.

Existing observations do not allow us to determine the peak time of the afterglow light curve. However, as long as the ambient density is at least $\sim 10^{-4} \text{ cm}^{-3}$ (a reasonable estimate, assuming the merger occurred within the interstellar or circumgalactic medium of the galaxy³⁸), we expect that emission from the core of the jet will become visible within at most $t \sim 1$ year after the merger and possibly sooner (see Supplementary Information). After the peak, the light curves across all frequency bands will plateau and then decay as a power law with an index between -1.1 and -2.1 , depending on whether the jet spreads sideways and when it ceases to be relativistic. This prediction is distinct from the mildly relativistic cocoon model, which predicts a longer rise and ultimately a shallower decay, as $t^{-0.8}$. We thus anticipate that it will be possible to determine the correct model in the near future.

Afterglows from structured jets, such as the one proposed here for GRB 170817A, brighten earlier than ‘top-hat’ jet models for off-axis observers. Therefore they imply an increase in the rate of orphan afterglows for deep optical surveys, $\gtrsim 23$ mag.³⁹ Assuming similar jet parameters to those estimated for GW170817, we expect short GRBs with energies typical of cosmological bursts (isotropic equivalent energies $\gtrsim 3 \times 10^{49}$ erg) to be associated with ~ 5 – 15% of binary neutron star gravitational-wave detections (cf. Ref³⁷). This accounts for gravitational-wave selection effects, which moderately favour nearly on-axis sources. The effective opening angle at which a structured jet such as the one proposed here could be observed at cosmological distances, ~ 10 degrees, yields a beaming factor of ~ 100 , broadly consistent with that inferred by observations.⁴⁰ This yields a true estimate of short GRB rates of order $1000 \text{ Gpc}^{-3} \text{ yr}^{-1}$, consistent with Galactic double neutron star observations⁴¹ and the rate inferred from GW170817.¹

In this model, an observer viewing down the axis of the merger would have observed a short GRB that is comparable in energy to those typically seen by γ -ray satellites. On the other hand, an observer at $\theta_{\text{obs}} = 20^\circ$ would be in a part of the jet with isotropic equivalent kinetic energy of $\sim 5 \times 10^{47}$ erg, consistent with the subluminal GRB 170817A.⁴² The range of jet energies directed toward the observer in structured jets could explain the puzzling diversity in observed short GRB luminosities.³³

Methods

Observations and reductions. Observations were taken with Wide Field Camera 3 (WFC3) on-board *Hubble Space Telescope* using both UVIS (F606W and F814W) and IR (F140W and F160W) channels. Each set of exposures was divided into 4 dithered pointings to allow for the use of image drizzling⁴³ in order to improve the spatial resolution. All processed frames were obtained from the *HST* data archive and drizzled to pixel scales of 0.025'' and 0.07'' for the UVIS and IR channels, respectively.

Astrometry and photometry. We determined the location of GW170817 in the images via relative astrometry using our *HST* observations taken at earlier epochs.^{10,18} Using 20–30 point sources in common to each pair of images, the geometric transformations achieve an rms ~ 0.1 – 0.2 pixels in each filter². Since the source lies at a small projected offset from its bright host galaxy, photometry requires the removal of the galaxy light. In principle this can be done simply by estimating the background light in a small aperture around the source position. However, in order to subtract the gradient of the galaxy light, we modelled the galaxy as a series of elliptical isophotes with the IRAF task `ellipse`. Prior to creating this model, point sources in the images were masked after automated detection with `SExtractor`.⁴⁴ The removal of such sources is required in order to afford an accurate determination of the galaxy’s underlying surface brightness profile when constructing the model. This isophotal model was subtracted from our images to yield a frame in which the galaxy background is removed. Although residuals were present in the inner regions where the morphology of NGC 4993 is complex¹⁸, at the location of GW170817 the background was smoothly subtracted. Aperture photometry was then performed in 0.08 and 0.15'' radii apertures (for UVIS and IR channels, respectively) using the local background to estimate the uncertainty and corrected according to the published WFC3 encircled energy curves. Finally we corrected for Galactic extinction in the direction of NGC 4993 of $E(B - V) = 0.105$ mag⁴⁵ using an $R = 3.1$ extinction law.⁴⁶ As a check of the method, we also made use of publicly available pre-merger *HST* imaging in order to perform image subtraction⁴⁷ to remove the galaxy background light. Pre-merger imaging is only available in F606W and is shallow (exposure time 696 seconds) compared to our imaging. After aligning and subtracting this template galaxy image we repeated our photometry method and found $m_{\text{F606W}} = 26.44 \pm 0.14$ mag. This image subtraction magnitude is in excellent agreement with our value determined by subtracting an elliptical isophote model as above ($m_{\text{F606W}} = 26.40 \pm 0.11$ mag), with a larger uncertainty due to the use of the comparatively noisy template image. We therefore report magnitudes in both F606W and F814W based on the removal of the model galaxy.

²As we do not have an early epoch of F140W image, this was tied to our earlier F110W image.

Supplementary Information

Off-axis afterglow constraints.

Here, we summarize the basic constraints that can be placed on the system parameters from the afterglow model. Our detailed model of a structured jet is presented in the following section.

Observationally, the emission from GW170817 at $\sim 108 - 110$ days after merger is broadly described by a spectral power law extending from radio through optical to X-ray frequencies, with $F_\nu \propto \nu^{-0.55}$ to $\nu^{-0.6}$. This spectral slope is consistent with that found from radio and X-ray observations at earlier times, although the uncertainties at ~ 15 days after merger are much larger. The optical observations at 110 days are marginally above this power-law, indicating that the synchrotron cooling frequency could be in the X-ray band at this time. A spectral power-law with a slope of -0.55 to -0.6 below the cooling break is consistent with a GRB afterglow with an electron energy distribution power-law slope $p \sim 2.1$ to 2.2 .^{48,49}

This robust power-law spectrum implies that all observational frequencies are within or close to the range between the synchrotron frequency of minimal energy electrons (which must be below the radio frequency, $\nu_m < 3$ GHz) and the cooling frequency (which must be above or not much below the X-ray frequency, $\nu_c \gtrsim 3.7 \times 10^{17}$ Hz). However, ν_m and ν_c depend on a number of parameters, including fractions of the internal energy in the electrons ϵ_e and in the magnetic field ϵ_B , and this requirement does not significantly constrain these beyond $\epsilon_B \lesssim 0.1$, $\epsilon_e \lesssim 0.01$.

The lack of a prompt X-ray signature,⁶ the dimness of the GRB itself,³ and the brightness and continuing rise of the radio and X-ray afterglow,^{12–14,26,50,51} indicate any relativistic jet, launched as part of the merger, is being viewed off-axis. However, these observational constraints have also been used to argue against the afterglow being due to an jet, instead possibly pointing to a more spherical cocoon of mildly-relativistic material as the source.^{12,13,30} This cocoon of material would be formed due to interaction between the jet and the ejecta from the merger. This merger interaction is favoured to have choked the jet in current cocoon interpretations for GW170817, resulting in no escape of a highly relativistic jet. For binary neutron star mergers, however, the amount of ejecta is small (a few hundredths of a solar mass was inferred for GW170817¹⁵), with a significant fraction in the binary plane,^{15,52–54} away from the polar direction of the jet. Therefore, it is not clear whether the jet can be choked or power a significant cocoon.³⁷

However, when considering the off-axis jet model, the relatively flat rise of the afterglow light curve argues against a single ‘top-hat’ jet with sharp edges. A top-hat jet would have a t^3 rise before peak luminosity, much steeper than the observed rise which scales at most linearly with time between ~ 10 and ~ 100 days after the merger. This argument has already been made on other grounds, such as the GRB itself: the relatively short delay time between the gravitational-wave signal and the GRB is inconsistent with moderately off-axis viewing unless the gamma-rays are emitted at very small radii, and the relationship between the observed gamma-ray flux and typical photon energies point to a relatively low-energy portion of the outflow being directed at the

observer⁴² (cf. Ref. ⁵⁵).

Whether the jet angular energy distribution is a top-hat or a Gaussian, as we consider in the following section, the observed flux will peak at a time when the observer located at angle θ_{obs} off-axis will be able to see the jet from the energetic on-axis core, i.e., when the jet core's Lorentz factor drops to $\Gamma \sim 1/\theta_{\text{obs}}$. If the jet expands sideways, this happens at⁵⁶

$$t_{\text{peak}} \approx 85 \left(\frac{n}{10^{-4} \text{ cm}^{-3}} \right)^{-1/3} \left(\frac{E_K}{10^{50} \text{ erg}} \right)^{1/3} \left(\frac{\theta_{\text{obs}}}{20 \text{ deg}} \right)^2 \text{ days}, \quad (1)$$

where E_K is the kinetic energy of the jet and n is the ambient density. Without sideways expansion, the light curve peaks more slowly, at

$$t_{\text{peak}} \approx 85 \left(\frac{n}{10^{-4} \text{ cm}^{-3}} \right)^{-1/3} \left(\frac{E_K}{10^{50} \text{ erg}} \right)^{1/3} \left(\frac{\theta_{\text{obs}}}{20 \text{ deg}} \right)^2 \left(\frac{\theta_{\text{obs}}}{\theta_0} \right)^{2/3} \text{ days}, \quad (2)$$

where θ_0 is the initial jet core opening angle. This can be expressed in terms of the isotropic-equivalent energy of the jet core, $E = 2E_K/\theta_0^2$, as

$$t_{\text{peak}} \approx 220 \left(\frac{n}{10^{-4} \text{ cm}^{-3}} \right)^{-1/3} \left(\frac{E}{3 \times 10^{52} \text{ erg}} \right)^{1/3} \left(\frac{\theta_{\text{obs}}}{20 \text{ deg}} \right)^{8/3} \text{ days}. \quad (3)$$

Here, we used fiducial values corresponding to the maximum isotropic-equivalent energy of observed on-axis GRBs and close to minimal halo ambient density⁵⁷. The maximum allowed inclination angle based on gravitational-wave data, the most recent Hubble constant measurements from the Dark Energy Survey, and the known redshift of the host galaxy NGC 4993 is $\theta_{\text{obs}} \leq 28^\circ$ at 90% confidence.^{1,58} Using this maximum observing angle extends the afterglow peak to 550 days.⁵⁸ Numerical simulations indicate that the light curves could peak somewhat later than in the analytical treatment.⁵⁶ On the other hand, it has been suggested⁴⁹ that these expressions should use $\Delta\theta \equiv \theta_{\text{obs}} - \theta_0$, the angle by which the observer is outside the jet core, in lieu of θ_{obs} , reducing the peak time. Therefore, we conclude that the light curve should reach the peak within ~ 1 year after the merger. Subsequently, the light curve from the post-jet-break off-axis jet will decay as $t^{-p} \sim t^{-2.1}$ if the jet expands sideways⁵⁶ or more slowly, as $\sim t^{3(1-p)/4-3/4} \sim t^{-1.6}$ if it does not.⁵⁹ The light curve decay will flatten to $\sim t^{-1.1}$ when the jet becomes non-relativistic and the outflow transitions to a Sedov-Taylor solution; it may therefore never reach the steeper $t^{-1.6} - t^{-2.1}$ decline if this transition happens soon after the peak. This is in contrast to the cocoon model, where there would be a longer continued rise and shallower decay afterwards, as $t^{3(1-p)/4} \sim t^{-0.8}$ in the relativistic regime, consistent with near-spherical ejecta.⁴⁹ Continued monitoring of the source to very late times will distinguish between the two scenarios.

The structured jet afterglow model. Here we consider a Gaussian structured jet as a model for the afterglow of GW170817; further details of the model are given in Ref ²⁵. Both the energy per solid angle and $\Gamma - 1$, where Γ is the bulk Lorentz factor, vary with angle from the central axis as

$\propto e^{-\theta^2/2\theta_0^2}$, where θ is the angle from the central-axis and θ_0 is the angular scale that defines the jet core. (Note that this corresponds to a low Lorentz factor for the portion of the jet directed toward the observer, which would therefore likely be opaque to prompt gamma rays⁵⁵; this may indicate a shallower Lorentz factor distribution across the jet.)

The numerical model splits the jet into a number of segments with a solid angle Ω . The flux contribution from each segment is calculated for an observer at an angle i from that segment's central axis. For an on-axis observer the segment flux is

$$F_\nu(t) = (L_\nu/4\pi D_L^2)(\Omega/\Omega_e), \quad (4)$$

where L_ν is the luminosity, D_L the luminosity distance, and $\Omega_e = \max[\Omega, \Omega_\Gamma]$. Here $\Omega_\Gamma = 2\pi(1 - \cos[1/\Gamma(\theta, t)])$ with t the time after deceleration. The flux from each of these small segments can be treated as a point source. For an off-axis observer at an inclination θ_{obs} from the jet central axis, or i from an individual jet segment, the flux becomes $F_\nu(t, i) = a^3 F_{\nu/a}(at, i = 0)$, where $a = \delta(i)/\delta(i = 0) < 1$, δ is the relativistic Doppler factor $[\Gamma(1 - \beta \cos i)]^{-1}$, and $\beta \equiv \sqrt{1 - \Gamma^{-2}}$.

There are a number of free parameters in the model, and the data do not constrain a unique solution. We present one set of parameters that provide a good match to the observations in Table 2. The light curve and spectra at ~ 15 and ~ 108 days, extracted to be roughly contemporaneous with the available afterglow data, are shown in Figure 3. The model spectra at ~ 15 days is a single power law with an index ~ -0.55 , indicating that the emission is between the synchrotron characteristic frequency, which must be $< 3 \times 10^9$ Hz, and the cooling frequency, which is $> 10^{18}$ Hz. At ~ 108 days, a break at $\sim 10^{17}$ Hz indicates the passage of the cooling frequency through the X-ray band. The index below the break is -0.55 and above the break ~ -1.05 .

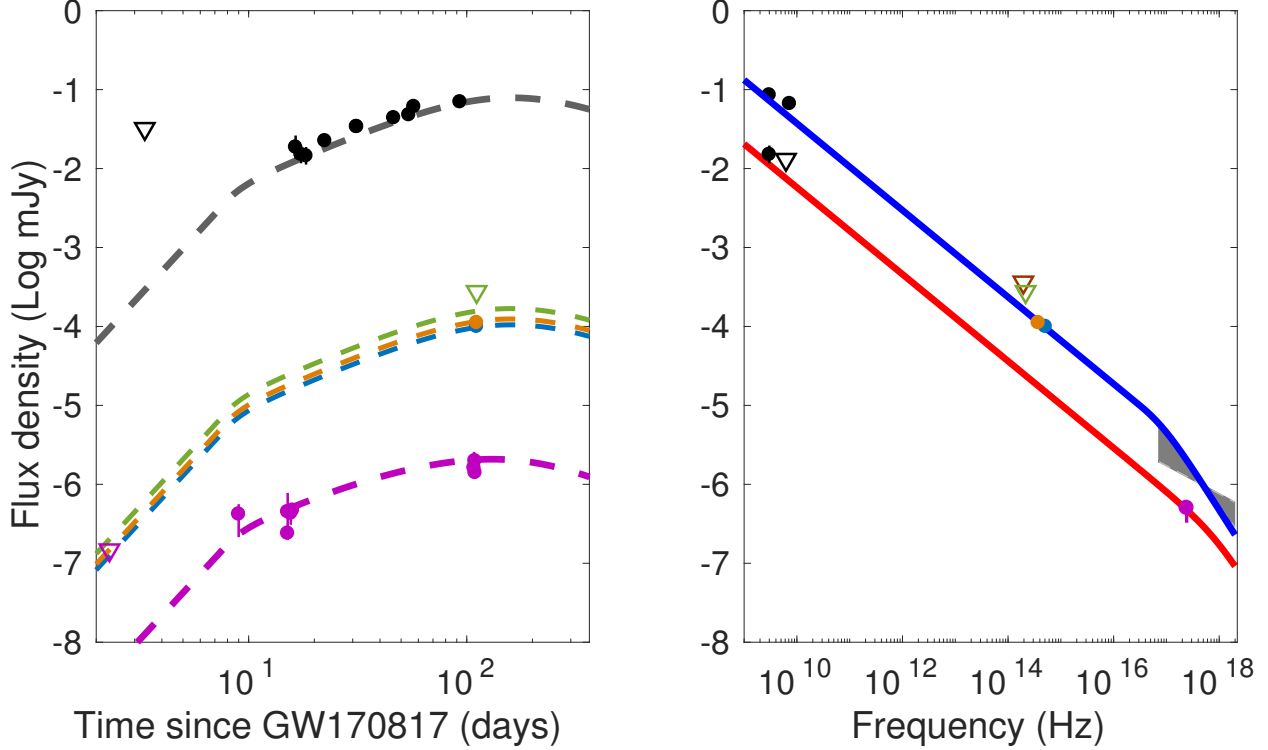


Figure 3 Light curve and spectra for Gaussian structured jet model. The current observed light curve and spectral energy distribution of the afterglow at radio, optical and X-ray wavelengths can be described by an off-axis structured jet. Left panel: Off-axis afterglow light-curve. Thick dashed grey and dashed purple lines indicate 3 GHz and 1 keV flux density respectively, overlaid with radio^{12,13} and X-ray data^{14,17,50,51}. Upper limits are shown as triangles. The green dashed line indicates *HST* near-IR F140W frequency while blue dashed and orange dashed lines show *HST* optical F606W and F814W fluxes. Our optical detections are indicated as error bars on the optical light curves and our near-IR flux limit is shown as an open triangle. Right panel: The model spectra at 14.9 days (red) and 108 days (blue) post-merger compared to radio^{12,13} and X-ray data^{14,17}. The X-ray flux at 15 days is shown at 1 keV as an error bar (see Methods). At 108 days, the X-ray data are shown as a spectral slope due to better spectral index constraints; the grey shaded region indicates the 1 σ bounds on the slope.¹⁴ Our optical detections at ~ 110 days are indicated by error bars. Uncertainties shown are 1 σ .

The first break in the model light-curve is the jet deceleration time for an off-axis observer, $t \propto E^{1/3} n^{-1/3} \Gamma^{-8/3} a^{-1}$, where before the break the flux is $\propto t^3$ and the jet is assumed not to expand sideways. A higher jet core Lorentz factor moves this break to earlier times. Each jet component will have a beaming angle equal to a given angle i at post-merger time $t \propto E^{1/3} n^{-1/3} i^{8/3}$ for an on-axis observer, $\theta_{\text{obs}} = 0$, or at a factor $a^{-1} = (1 - \beta \cos i)/(1 - \beta) \sim 2$ of the on-axis time for an off-axis observer at an inclination $i = \Gamma^{-1}$. Here $E = 2E_K \theta_0^{-2}$ is the

isotropic equivalent jet kinetic energy of the component, and n is the ambient number density. For wider jet components with a low Lorentz factor, emission can be beamed towards an observer before the jet starts to decelerate. After this time, flux from the more energetic and faster components is beamed towards the observer.

We do not yet know when the emission will reach its peak; our parameters are chosen so that a ‘top-hat’ jet with the core parameters of the Gaussian jet model and without lateral expansion or limb brightening, would yield a peak at ~ 140 days for an observer at the model inclination of $\theta_{\text{obs}} = 20^\circ$. Lateral expansion will reduce the peak time, while significant limb brightening will add to the flux after the peak for off-axis observers. The late time flux decline approaches the ‘on-axis’ post jet-break flux, for our parameters, without sideways expansion, as $\propto t^{-1.6}$. At very late times when the jet becomes non-relativistic the decline will transition from the steep Blandford-McKee solution to a Sedov-Taylor solution, $t^{-1.1}$. At this point the receding counter-jet will become observable, resulting in a bump in the afterglow decline. Late-time, ~ 2 years post-merger, radio observations may be able to reveal this feature.

Optical detections as being due to an underlying, unrelated source. Given the depth of our observations, and the relative proximity of NGC 4993, the absolute magnitude we are sensitive to at the location of GW170817 ($\gtrsim -6$ mag) probes well down the luminosity function of typical globular cluster (GC) or young star cluster populations (e.g. the average Galactic GC luminosity is ~ -8 mag⁶⁰). As such we consider the possibility that our detections are due to an unrelated source. Firstly, we assessed the presence of any offset between our new detections and earlier *HST* epoch detections of the kilonova light. We were able to determine a relative astrometric transformation with a 0.1–0.2 pixels r.m.s. ($\sim 2.5 - 5$ mas, or $\sim 0.5 - 1$ pc at the distance of NGC 4993). However, owing to the relative faintness of our new detections, our main source of uncertainty was the centroiding of the source itself. Although this can be estimated as $\frac{\text{FWHM}}{2.35 \times \text{SNR}}$, practically we were also subject to uncertainties based on our choice of method to centre the faint source. The centre uncertainties were $\sim 2 - 3$ pc (the uncertainty in the centre of the source in our earlier epochs was negligible owing to the much higher significance of those detections). When considering our sources of uncertainty, we find the new sources have no significant offset from our earlier epoch detections. Secondly, we consider the colour of the new detections. The source is relatively blue, at $F606W - F814W = 0.11 \pm 0.21$ mag, when compared to GCs, which typically have ~ 0.5 mag in the same colour.^{61,62} However, the large uncertainty on the colour of our detection precludes strong statements when comparing to colours of GCs. In Figure 4 we show the GC population of the nearby elliptical galaxy M87 ($D_L \simeq 16.5$ Mpc) in comparison to our detection.⁶³ We also find a lack of other similarly blue sources within NGC 4993 – this is consistent with the S0 classification and studies showing a lack of recent star-formation in the galaxy.^{18,64,65} Additionally, we note that no source was found in the pre-existing *HST* imaging of the merger site in F606W, although these data were shallower in depth than our observations.^{8,18,64} Our F606W subtraction against the pre-imaging of the galaxy (see Methods) still reveals the source, suggesting that it was not present in the pre-imaging observations, even at a marginal level, and supports its interpretation as a transient source. Although binary neutron-stars may be dynamically formed in dense stellar clusters,⁶⁶ the natal kicks imparted to the neutron stars at birth are significantly

larger than the escape velocity of such clusters (few tens of km s^{-1}). As such, there is no reason to expect the presence of a stellar cluster underlying the merger site (above that expected for a random location at similar offset in the host), even in the dynamically-formed scenario. Given the above arguments and the consistency of our detections with power-law models of the afterglow emission from radio and X-ray data, we consider that our detections are indeed due to the transient for the purposes of this study. However, continued long-term optical monitoring of the source alongside radio and X-ray observations is required to conclusively rule on whether the emission is due to an unrelated, underlying source. In such case we would not expect any significant change in the observed flux, unlike the evolving optical light curve expected for an afterglow model.

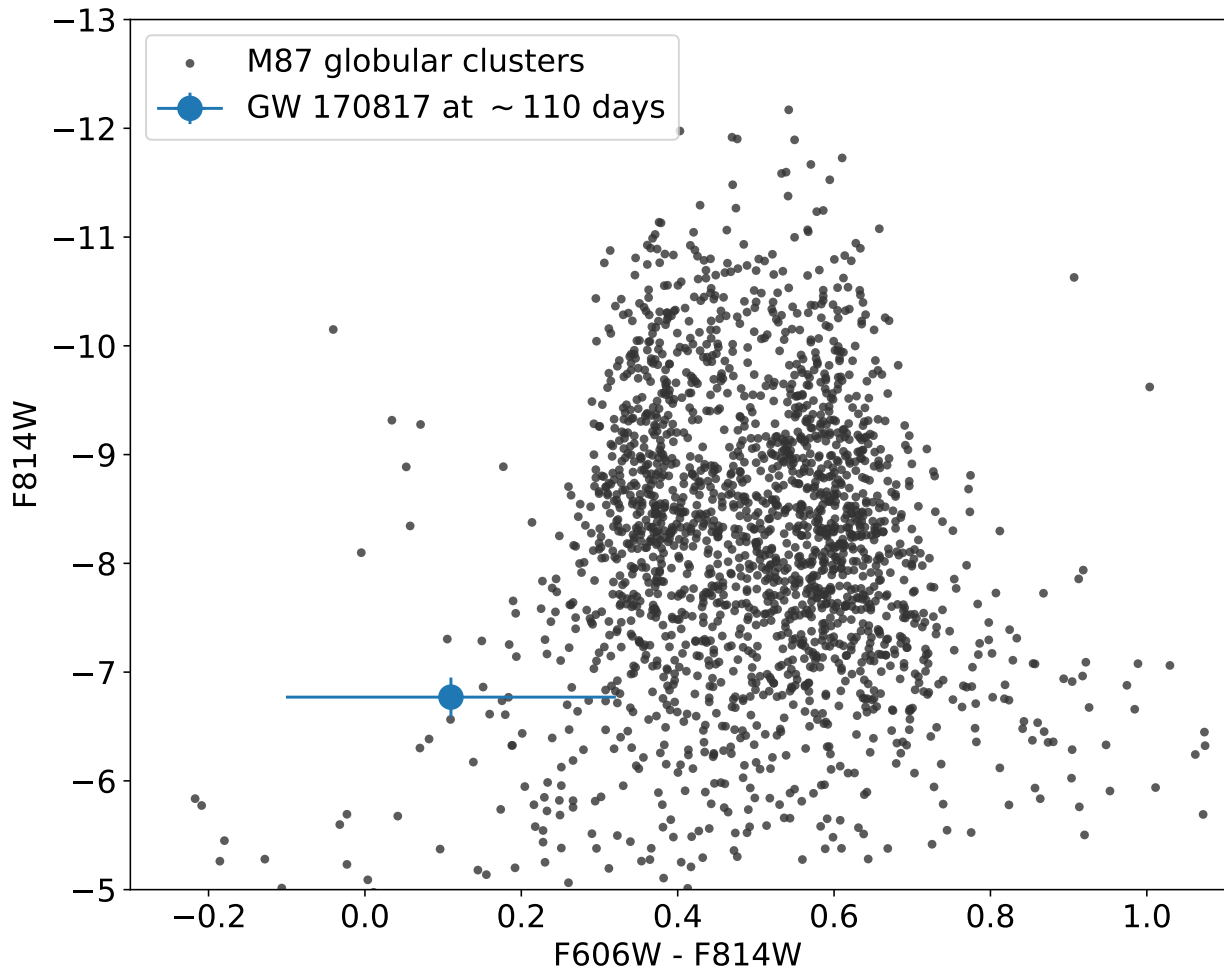


Figure 4 Colour-magnitude diagram of GW170817 at late times and globular clusters of M87. We consider the possibility that our late-time detections are due to an underlying globular cluster. The optical colour of our detection of GW170817 (blue, large marker) appears bluer than the globular cluster population of early type galaxies (shown here for M87, small dark markers), although our large uncertainty on the colour means

it cannot be significantly distinguished from a population of globular cluster colours. Uncertainties shown for GW170817 are 1σ . The globular cluster data⁶³ have been trimmed to show only those with a 1σ uncertainty in $F606W - F814W$ of < 0.1 mag – individual uncertainty bars are not shown for clarity.

1. Abbott, B. P. *et al.* GW170817: Observation of Gravitational Waves from a Binary Neutron Star Inspiral. *Physical Review Letters* **119**, 161101 (2017). 1710.05832.
2. Abbott, B. P. *et al.* Multi-messenger Observations of a Binary Neutron Star Merger. *ApJ* **848**, L12 (2017). 1710.05833.
3. Abbott, B. P. *et al.* Gravitational Waves and Gamma-Rays from a Binary Neutron Star Merger: GW170817 and GRB 170817A. *ApJ* **848**, L13 (2017). 1710.05834.
4. Arcavi, I. *et al.* Optical emission from a kilonova following a gravitational-wave-detected neutron-star merger. *Nature* **551**, 64–66 (2017). 1710.05843.
5. Coulter, D. A. *et al.* Swope Supernova Survey 2017a (SSS17a), the Optical Counterpart to a Gravitational Wave Source. *ArXiv e-prints* (2017). 1710.05452.
6. Evans, P. A. *et al.* Swift and NuSTAR observations of GW170817: detection of a blue kilonova. *ArXiv e-prints* (2017). 1710.05437.
7. Pian, E. *et al.* Spectroscopic identification of r-process nucleosynthesis in a double neutron-star merger. *Nature* **551**, 67–70 (2017). 1710.05858.
8. Smartt, S. J. *et al.* A kilonova as the electromagnetic counterpart to a gravitational-wave source. *Nature* **551**, 75–79 (2017). 1710.05841.
9. Soares-Santos, M. *et al.* The Electromagnetic Counterpart of the Binary Neutron Star Merger LIGO/Virgo GW170817. I. Discovery of the Optical Counterpart Using the Dark Energy Camera. *ApJ* **848**, L16 (2017). 1710.05459.
10. Tanvir, N. R. *et al.* The Emergence of a Lanthanide-rich Kilonova Following the Merger of Two Neutron Stars. *ApJ* **848**, L27 (2017). 1710.05455.
11. Valenti, S. *et al.* The Discovery of the Electromagnetic Counterpart of GW170817: Kilonova AT 2017gfo/DLT17ck. *ApJ* **848**, L24 (2017). 1710.05854.
12. Hallinan, G. *et al.* A Radio Counterpart to a Neutron Star Merger. *ArXiv e-prints* (2017). 1710.05435.
13. Mooley, K. P. *et al.* A mildly relativistic wide-angle outflow in the neutron star merger GW170817. *ArXiv e-prints* (2017). 1711.11573.
14. Ruan, J. J., Nynka, M., Haggard, D., Kalogera, V. & Evans, P. Brightening X-ray Emission from GW170817/GRB170817A: Further Evidence for an Outflow. *ArXiv e-prints* (2017). 1712.02809.
15. Kasen, D., Metzger, B., Barnes, J., Quataert, E. & Ramirez-Ruiz, E. Origin of the heavy elements in binary neutron-star mergers from a gravitational-wave event. *Nature* **551**, 80–84 (2017). 1710.05463.

16. Waxman, E., Ofek, E., Kushnir, D. & Gal-Yam, A. Constraints on the ejecta of the GW170817 neutron-star merger from its electromagnetic emission. *ArXiv e-prints* (2017). 1711.09638.
17. Haggard, D. *et al.* A Deep Chandra X-Ray Study of Neutron Star Coalescence GW170817. *ApJ* **848**, L25 (2017). 1710.05852.
18. Levan, A. J. *et al.* The Environment of the Binary Neutron Star Merger GW170817. *ApJ* **848**, L28 (2017). 1710.05444.
19. Rosswog, S. *et al.* Detectability of compact binary merger macronovae. *Classical and Quantum Gravity* **34**, 104001 (2017). 1611.09822.
20. Drout, M. R. *et al.* Light Curves of the Neutron Star Merger GW170817/SSS17a: Implications for R-Process Nucleosynthesis. *ArXiv e-prints* (2017). 1710.05443.
21. Gottlieb, O., Nakar, E., Piran, T. & Hotokezaka, K. A cocoon shock breakout as the origin of the γ -ray emission in GW170817. *ArXiv e-prints* (2017). 1710.05896.
22. Kumar, P. & Granot, J. The Evolution of a Structured Relativistic Jet and Gamma-Ray Burst Afterglow Light Curves. *ApJ* **591**, 1075–1085 (2003). astro-ph/0303174.
23. Zhang, B., Dai, X., Lloyd-Ronning, N. M. & Mészáros, P. Quasi-universal Gaussian Jets: A Unified Picture for Gamma-Ray Bursts and X-Ray Flashes. *ApJ* **601**, L119–L122 (2004). astro-ph/0311190.
24. Salafia, O. S., Ghisellini, G., Pescalli, A., Ghirlanda, G. & Nappo, F. Structure of gamma-ray burst jets: intrinsic versus apparent properties. *MNRAS* **450**, 3549–3558 (2015). 1502.06608.
25. Lamb, G. P. & Kobayashi, S. Electromagnetic counterparts to structured jets from gravitational wave detected mergers. *MNRAS* **472**, 4953–4964 (2017). 1706.03000.
26. Kim, S. *et al.* ALMA and GMRT constraints on the off-axis gamma-ray burst 170817A from the binary neutron star merger GW170817. *ArXiv e-prints* (2017). 1710.05847.
27. Bazin, G. *et al.* The core-collapse rate from the Supernova Legacy Survey. *A&A* **499**, 653–660 (2009). 0904.1066.
28. Gompertz, B. P. *et al.* The Diversity of Kilonova Emission in Short Gamma-Ray Bursts. *ArXiv e-prints* (2017). 1710.05442.
29. Cowperthwaite, P. S. *et al.* The Electromagnetic Counterpart of the Binary Neutron Star Merger LIGO/Virgo GW170817. II. UV, Optical, and Near-infrared Light Curves and Comparison to Kilonova Models. *ApJ* **848**, L17 (2017). 1710.05840.
30. Kasliwal, M. M. *et al.* Illuminating Gravitational Waves: A Concordant Picture of Photons from a Neutron Star Merger. *ArXiv e-prints* (2017). 1710.05436.

31. Lipunov, V. M. *et al.* MASTER Optical Detection of the First LIGO/Virgo Neutron Star Binary Merger GW170817. *ApJ* **850**, L1 (2017). 1710.05461.
32. Guillochon, J., Parrent, J., Kelley, L. Z. & Margutti, R. An Open Catalog for Supernova Data. *ApJ* **835**, 64 (2017). 1605.01054.
33. Berger, E. Short-Duration Gamma-Ray Bursts. *ARA&A* **52**, 43–105 (2014). 1311.2603.
34. Ruiz, M., Lang, R. N., Paschalidis, V. & Shapiro, S. L. Binary Neutron Star Mergers: A Jet Engine for Short Gamma-Ray Bursts. *ApJ* **824**, L6 (2016). 1604.02455.
35. Perego, A. *et al.* Neutrino-driven winds from neutron star merger remnants. *MNRAS* **443**, 3134–3156 (2014). 1405.6730.
36. Bromberg, O., Nakar, E., Piran, T. & Sari, R. The Propagation of Relativistic Jets in External Media. *ApJ* **740**, 100 (2011). 1107.1326.
37. Lazzati, D. *et al.* Late time afterglow observations reveal a collimated relativistic jet in the ejecta of the binary neutron star merger GW170817. *ArXiv e-prints* (2017). 1712.03237.
38. Oppenheimer, B. D. *et al.* Bimodality of low-redshift circumgalactic O VI in non-equilibrium EAGLE zoom simulations. *MNRAS* **460**, 2157–2179 (2016). 1603.05984.
39. Lamb, G. P., Tanaka, M. & Kobayashi, S. Transient Survey Rates for Orphan Afterglows from Compact Merger Jets. *ArXiv e-prints* (2017). 1712.00418.
40. Fong, W. *et al.* A Jet Break in the X-Ray Light Curve of Short GRB 111020A: Implications for Energetics and Rates. *ApJ* **756**, 189 (2012). 1204.5475.
41. Abadie, J. *et al.* Predictions for the Rates of Compact Binary Coalescences Observable by Ground-based Gravitational-wave Detectors. *Classical and Quantum Gravity* **27**, 173001–+ (2010). 1003.2480.
42. Granot, J., Guetta, D. & Gill, R. Lessons from the Short GRB 170817A: The First Gravitational-wave Detection of a Binary Neutron Star Merger. *ApJ* **850**, L24 (2017). 1710.06407.
43. Fruchter, A. S. & Hook, R. N. Drizzle: A Method for the Linear Reconstruction of Under-sampled Images. *PASP* **114**, 144–152 (2002). astro-ph/9808087.
44. Bertin, E. & Arnouts, S. SExtractor: Software for source extraction. *A&A Supp* **117**, 393–404 (1996).
45. Schlafly, E. F. & Finkbeiner, D. P. Measuring Reddening with Sloan Digital Sky Survey Stellar Spectra and Recalibrating SFD. *ApJ* **737**, 103 (2011). 1012.4804.
46. Fitzpatrick, E. L. Correcting for the Effects of Interstellar Extinction. *PASP* **111**, 63–75 (1999). arXiv:astro-ph/9809387.

47. Alard, C. Image subtraction using a space-varying kernel. *A&A Supp* **144**, 363–370 (2000).
48. Sari, R., Piran, T. & Narayan, R. Spectra and Light Curves of Gamma-Ray Burst Afterglows. *ApJ* **497**, L17–L20 (1998). [astro-ph/9712005](#).
49. Granot, J. & Sari, R. The Shape of Spectral Breaks in Gamma-Ray Burst Afterglows. *ApJ* **568**, 820–829 (2002). [astro-ph/0108027](#).
50. Troja, E. *et al.* The X-ray counterpart to the gravitational-wave event GW170817. *Nature* **551**, 71–74 (2017). [1710.05433](#).
51. Margutti, R. *et al.* The Electromagnetic Counterpart of the Binary Neutron Star Merger LIGO/Virgo GW170817. V. Rising X-Ray Emission from an Off-axis Jet. *ApJ* **848**, L20 (2017). [1710.05431](#).
52. Metzger, B. D. *et al.* Electromagnetic counterparts of compact object mergers powered by the radioactive decay of r-process nuclei. *MNRAS* **406**, 2650–2662 (2010). [1001.5029](#).
53. Tanaka, M. *et al.* Kilonova from post-merger ejecta as an optical and near-infrared counterpart of GW170817. *ArXiv e-prints* (2017). [1710.05850](#).
54. Shibata, M. *et al.* Modeling GW170817 based on numerical relativity and its implications. *ArXiv e-prints* (2017). [1710.07579](#).
55. Kisaka, S., Ioka, K., Kashiyama, K. & Nakamura, T. Scattered Short Gamma-Ray Bursts as Electromagnetic Counterparts to Gravitational Waves and Implications of GW170817 and GRB 170817A. *ArXiv e-prints* (2017). [1711.00243](#).
56. Granot, J., Gill, R., Guetta, D. & De Colle, F. Off-Axis Emission of Short GRB Jets from Double Neutron Star Mergers and GRB 170817A. *ArXiv e-prints* (2017). [1710.06421](#).
57. Fong, W., Berger, E., Margutti, R. & Zauderer, B. A. A Decade of Short-duration Gamma-Ray Burst Broadband Afterglows: Energetics, Circumburst Densities, and Jet Opening Angles. *ApJ* **815**, 102 (2015). [1509.02922](#).
58. Mandel, I. The orbit of GW170817 was inclined by less than 28 degrees to the line of sight. *ArXiv e-prints* (2017). [1712.03958](#).
59. Panaitescu, A. & Mészáros, P. Dynamical Evolution, Light Curves, and Spectra of Spherical and Collimated Gamma-Ray Burst Remnants. *ApJ* **526**, 707–715 (1999). [astro-ph/9806016](#).
60. Harris, W. E. A Catalog of Parameters for Globular Clusters in the Milky Way. *AJ* **112**, 1487 (1996).
61. Madrid, J. P., Harris, W. E., Blakeslee, J. P. & Gómez, M. Structural Parameters of the Messier 87 Globular Clusters. *ApJ* **705**, 237–244 (2009). [0909.0272](#).

62. Carlson, N. L. *et al.* Globular cluster population of the HST frontier fields galaxy J07173724+3744224. *ArXiv e-prints* (2017). 1711.09500.
63. Peng, E. W. *et al.* The Color-Magnitude Relation for Metal-Poor Globular Clusters in M87: Confirmation from Deep HST/ACS Imaging. *ApJ* **703**, 42–51 (2009). 0907.2524.
64. Blanchard, P. K. *et al.* The Electromagnetic Counterpart of the Binary Neutron Star Merger LIGO/Virgo GW170817. VII. Properties of the Host Galaxy and Constraints on the Merger Timescale. *ApJ* **848**, L22 (2017). 1710.05458.
65. Im, M. *et al.* Distance and Properties of NGC 4993 as the Host Galaxy of the Gravitational-wave Source GW170817. *ApJ* **849**, L16 (2017). 1710.05861.
66. Davies, M. B. The binary zoo: the calculation of production rates of binaries through 2+1 encounters in globular clusters. *MNRAS* **276**, 887–905 (1995). astro-ph/9507026.

Acknowledgements Based on observations made with the NASA/ESA Hubble Space Telescope, obtained from the data archive at the Space Telescope Science Institute. STScI is operated by the Association of Universities for Research in Astronomy, Inc. under NASA contract NAS 5-26555. These observations are associated with programs GO 14771 (Tanvir), GO 14270 (Levan). We thank the staff at STScI for their excellent support of these observations. AJL acknowledges that this project has received funding from the European Research Council (ERC) under the European Union’s Horizon 2020 research and innovation programme (grant agreement no 725246). AJL, DS, KW, JDL acknowledge support from STFC via grant ST/P000495/1. NRT, PTO, JPO, GPL, IM, SK acknowledge support from STFC. GPL acknowledges partial support from RAS and IAU grants JH was supported by a VILLUM FONDEN Investigator grant (project number 16599). AdUP, CT and ZC acknowledge support from the Spanish project AYA 2014-58381-P. ZC also acknowledges support from the Juan de la Cierva Incorporación fellowship IJCI-2014-21669. MI acknowledges the support from the NRFK grant, No. 2017R1A3A3001362. SR has been supported by the Swedish Research Council (VR) under grant number 2016- 03657_3, by the Swedish National Space Board under grant number Dnr. 107/16 and by the research environment grant “Gravitational Radiation and Electromagnetic Astrophysical Transients (GREAT)” funded by the Swedish Research council (VR) under Dnr 2016-06012. PAE acknowledges UKSA support. DJW is supported by the the Danish Agency for Science, Technology and Innovation under grant number DFF 7014-00017. GPL and SK thank Ehud Nakar for helpful comments. IM thanks Jonathan Granot for useful discussions.

Author Contributions JDL performed the data reduction and analysis and led writing of the manuscript. GPL performed the numerical calculations and wrote text relating to the model. IM contributed to theoretical interpretation of the data and provided analytical estimates. AJL and NRT are PIs of the *HST* proposals used to obtain the new data presented and assisted with data analysis and text. SK assisted with the development of the model. BG and JH contributed to the interpretation of the data and performed the phenomenological fits. ASF and TK performed the image subtraction test. All authors provided comments and analysis to assist in the writing of the observing proposals and manuscript.

Competing Interests The authors declare that they have no competing financial interests.

Correspondence Correspondence and requests for materials should be addressed to JDL (email: J.D.Lyman@warwick.ac.uk).

Obs. date (MJD)	Rest-frame epoch (days)	Instrument	Filter	Exp. time (s)	AB Mag
58093.007	109.41	WFC3/UVIS	F606W	2264	26.40 ± 0.11
58093.074	109.47	WFC3/IR	F160W	2397	>25.0
58093.139	109.54	WFC3/UVIS	F814W	2400	26.29 ± 0.18
58093.206	109.61	WFC3/IR	F140W	4794	>25.3

Table 1: **Log of late time *HST* observations of GW170817.** Epochs for observations are given as time since the gravitational wave signal (correct for the source’s redshift of $z = 0.007983$). Magnitudes have been corrected for Galactic extinction using $E(B-V) = 0.105$ mag. Uncertainties are 1σ and limits in the IR channel are given as 3σ .

Model Parameter	Description	Value
E	Isotropic equivalent kinetic energy	1.0×10^{52} erg
Γ	Initial bulk Lorentz factor	60
n	Ambient density	1.3×10^{-3} cm $^{-3}$
ε_e	Electron energy fraction	0.01
ε_B	Magnetic field energy fraction	0.01
p	Electron energy distribution	2.1
θ_c	Opening angle of jet core	4.5°
θ_{obs}	Observing angle	20°
D_L	Luminosity distance	41 Mpc

Table 2: **Model parameters for Gaussian structured jet.** The values for E and Γ are for the most energetic jet core. Some of the parameters are significantly correlated, and other combinations of parameter values can yield equally good fits to the observed data; e.g., the bulk Lorentz center is only constrained to $\Gamma \geq 60$. Values for parameters such as θ_{obs} and D_L were driven by constraints from the gravitational wave and electromagnetic observations.